Journal of the Korean Nuclear Society
Volume 31, Number 4, pp.408~422, August 1999

Investigating the Fluence Reduction Option for Reactor Pressure Vessel Lifetime Extension

Jong Kyung Kim, Chang Ho Shin, and Bo Kyun Seo
Hanyang University
17 Haengdang, Sungdong, Seoul 133-791, Korea
gemini@nural.hanyang.ac.kr

Myung Hyun Kim and Dong Kyu Kim
Kyunghee University
Kiheung, Yongin 449-701, Korea

Goung Jin Lee and Su Jin Oh
Chosun University
375, Seosuk, Dong, Kwangju 501-759, Korea

(Received March 25, 1999)

Abstract

To reduce the fast neutron fluence which deteriorates the RPV integrity, additional shields were assumed to be installed at the outer core structures of the Kori Unit 1 reactor, and its reduction effects were examined. Full scope Monte Carlo simulation with MCNP4A code was made to estimate the fast neutron fluence at the RPV. An optimized design option was found from various choices in geometry and material for shield structure. It was expected that magnitude of fast neutron fluence would be reduced by 39% at the circumferential weld of the RPV, resulting in extension of plant lifetime by 4.6 EFPYs based on the criterion of PTS requirement. It was investigated that the nuclear characteristics and thermal hydraulic factors at the internal core were only negligibly influenced by the installation of additional shield structure.

Key Words : reactor pressure vessel, vessel lifetime integrity, fast neutron fluence, monte carlo method

1. Introduction

Currently, many commercial nuclear power plants (NPP), all over the world are approaching the end of their design lifetime. In the early stages of development of the NPP industry, a

vast amount of effort was devoted to accumulating technology and experience related to plant construction. However, as the operating years of plants grow and the public concern over nuclear safety increases, plant aging and maintenance problems become a more significant matter of concern in the NPP industry.

The lifetime of a NPP is strongly related to the retention of the structural integrity of the reactor pressure vessel (RPV). The aging mechanism of primary concern for RPVs is irradiation-induced embrittlement of material at the vessel beltline. Irradiation embrittlement decreases not only the cleavage fracture toughness but also ductile tearing toughness of RPV materials [1]. Most of all, the neutrons with energies greater than approximately 1 MeV are the primary cause of RPV embrittlement. Therefore, if the fast neutron fluence at the RPV is effectively reduced by appropriate treatments, vessel integrity will then be ensured beyond the lifetime, and extended lifetime can be produced.

There are several fluence reduction options such as use of low leakage loading pattern, insertion of dummy assemblies at the core periphery, installation of additional shields at vessel internal structures, and power level derating [2]. Currently, most utilities including the Korea Electric Power Corporation (KEPCO) are implementing the low leakage schemes to decrease both fuel cycle costs and fast neutron fluence at the vessels. Among the several options, additional shield installation is expected to be easily applicable to the reactors. Furthermore, it would not cause remarkable changes in core characteristics and also would not cause loss of power generation capacity.

In this study, additional shield insertions were assumed to be applied to the outer core structures, and fluence reduction effect was examined in detail by using the Monte Carlo simulation. The changes of nuclear characteristics and thermal hydraulic factors due to additional shield insertion were analyzed, and the effectiveness of lifetime extension was evaluated quantitatively.

2. Methodology

2.1. Neutron Fluence Calculation at RPV

The Discrete Ordinates Method is generally used for the calculation of RPV fluence. This method is used to determine a synthesized three-dimensional flux distribution based on one-dimensional and two-dimensional transport calculations. This SN transport calculation contains uncertainties associated with the multigroup cross-section libraries, multi-dimensionality, geometric approximations, and angular discretization [3,4]. Recently, it has been recognized that an alternative method, the Monte Carlo, is available for accurate results.

Monte Carlo analysis of the neutronic behavior of a light water reactor (LWR) in combination with continuous cross-section data is an attractive tool which provides a detailed description of a static LWR core. Very few limitations exist in the area of geometric modeling. Furthermore, details of the original nuclear data evaluation can be retained in the cross-section library, and self-shielding in the resolved resonance range is explicitly taken into account. In recent days, the calculations of RPV fluence and criticality benchmark were performed by using the Monte Carlo Method, and the accuracy and consistency of this method was well established by previous workers [4-9]. Therefore, for an accurate estimate of the neutron fluence at the RPV and a reasonable description of outer fuel assemblies which is the critical source for RPV fluence, the

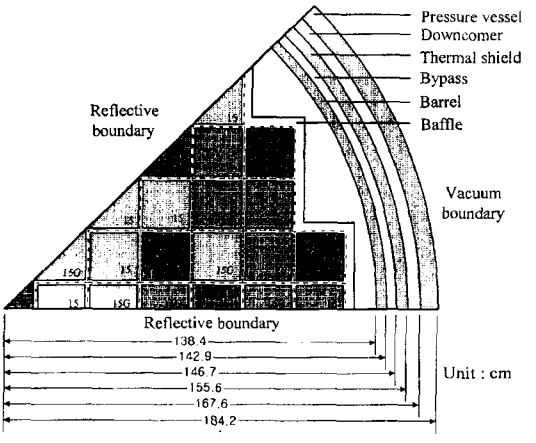

Fig. 1. Cross-Sectional View of the Kori Unit 1 Core

Monte Carlo simulation is well suited for this task and was used.

2.2. MCNP Model of Kori Unit 1

The Kori Unit 1 is a nuclear power plant constructed by KEPCO, which utilizes a Westinghouse nuclear steam supply system. The unit is designed to produce 1723.5 MW thermal core power [10]. The Kori Unit 1 reactor was chosen in this study because it is the first commercial nuclear power plant built in Korea, and life extension of the plant is being considered by KEPCO.

Figure 1 shows the cross-sectional view of one-eighth of the Kori Unit 1 reactor in-vessel components with reflective angular boundaries at 0 and 45 degrees, as modeled by MCNP4A [11]. This model explicitly represents the rectangular and cylindrical domains in three dimensions, and baffle, barrel, thermal shield, and pressure vessel were described clearly. The state of beginning of cycle life (BOL) in cycle 14 was simulated with hot full power (HFP) and all rods out (ARO)

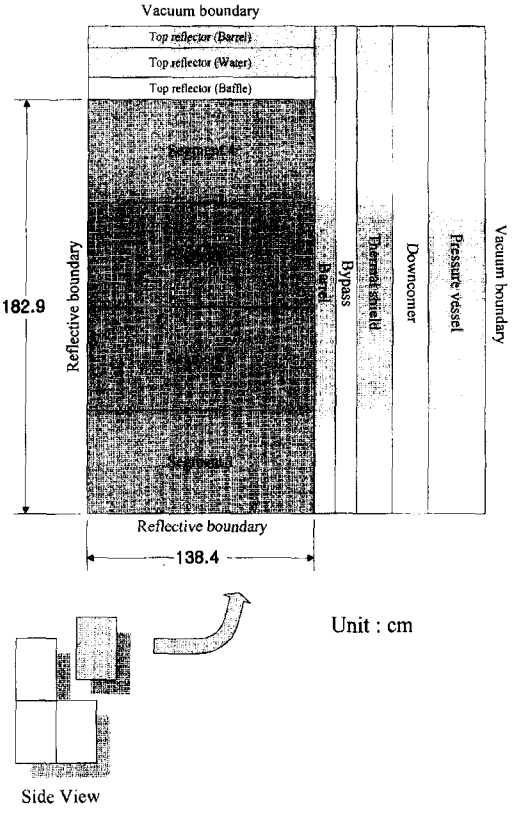

Fig. 2. Axial View of the Kori Unit 1 Core

conditions. Figure 2 shows the axial view of one-second of the reactor with reflective boundary at the core center. To estimate the axial power distributions in the fuel rod, each assembly was divided into 4 segments at the axial direction. Top reflector was assumed by three layers of baffle, coolant, and barrel as in the side reflector region. Reflective geometry (one-sixteenth core modeled) reduced the size of the input model, allowing code run to be faster.

To model the cycle 14 core configurations, it is necessary to have uranium, plutonium, and fission product concentrations for representation of the depleted core. For this information, associated depletion calculations were performed by CASMO-3 code [12]. The isotopic

inventories in each assembly at their burnup steps were generated and used by MCNP material input. For the purpose of considering the Doppler broadening effect, a new cross-section library was generated at the core temperature by NJOY [13] and ENDF/B-VI. In this study, the methods chosen to accelerate tally convergence were energy cutoff, geometry splitting with Russian roulette, and weight cutoff. In general, only neutrons with energies above 1 MeV are considered to contribute metal damage [14], thus this energy was chosen for cutoff-energy in the RPV fluence calculations.

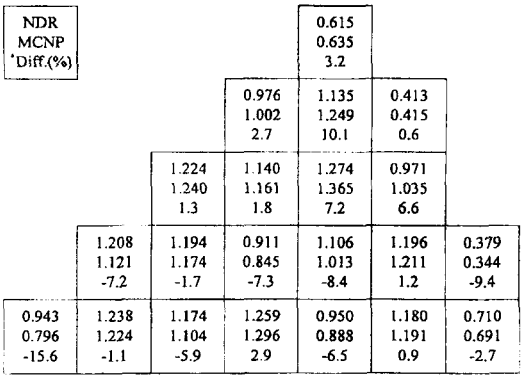

*Difference(%) = (MCNP-NDR)/NDR×100

Fig. 2. Relative Assembly Power Distribution of the Reference Reactor Model

2.3. Results of Normal Operation

A couple of calculations were carried out to estimate fast neutron fluence at the RPV. One is a criticality calculation, and the other is a fluence calculation. The criticality calculation employs the KCODE option [11] to obtain keff eigenvalue of the system and relative power distributions. In the reference model of the Kori Unit 1 cycle 14, by confirming that keff was converged to unity and relative power distribution was consistent with that of the Nuclear Design Report (NDR) [15], the validity of the model was examined.

In four segments of each fuel rod, fission reaction densities were calculated. These results were used as neutron source information for RPV fluence calculations. After 150 cycle calculations (KCODE), the reference system converged to a keff value of $0.99690^{\circ} \pm 0.00074$. While the criticality calculation was performed, the relative pin power calculations in all rods of the four segments were carried out. Thereafter, the averaged relative assembly power was calculated from the integrated pin powers. Figure 3 shows the relative assembly power distribution together with the values of the NDR data of the Kori Unit 1 cycle 14.

The relative pin power distributions in all rods of the four segments from the previous criticality calculation were converted to the neutron source probabilities in the RPV fluence calculation. By the fixed source problem (SDEF) [11] of MCNP, the probability distribution function of the source was established such that the probability of a neutron starting in a segment of a rod was proportional to the normalized power fraction of that segment. Once the position of a starting neutron was determined, its energy was selected from the Watt fission spectrum of the fissile nuclides.

The pressure vessel of the Kori Unit 1 was fabricated with SA508 class 2 forging and Linde 80 flux circumferential welds as shown in Figure 4. The welds undergo more severe irradiation embrittlement because of their high-copper and -nickel contents. Among the welds of the vessel, the weld situated at 37.5 cm from the core center was highly damaged by fast neutron bombard-ments. Tally region was set around this high-flux weld line, and that was subdivided into 18 sub-cells by 2.5 degrees along the azimuth. The angular fast neutron fluence (E>1 MeV)

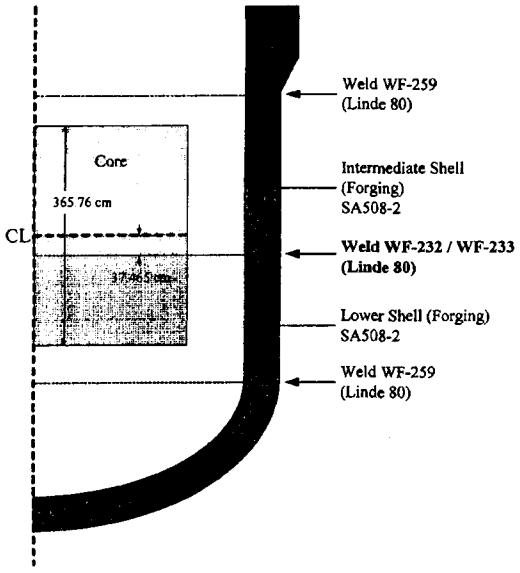

Fig. 4. Pressure Vessel of the Kori Unit 1 Reactor

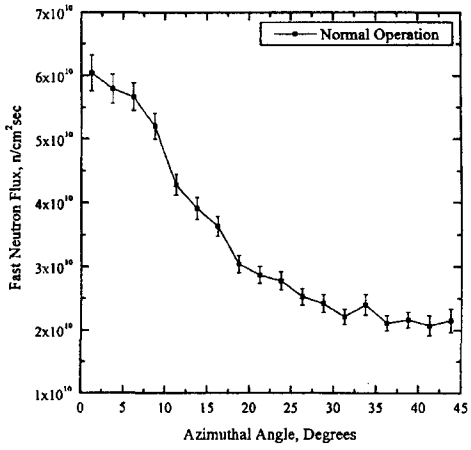

Fig. 5. Angular Fluence Distribution of the Reference Model

distribution at the weld of the reference core is described in Figure 5. After the sufficient neutron transport simulations with ten million histories were done, the relative error of all tallies was achieved within 5%. It is noted that the weld flux shows a peak at 0 degree, due to core geometry and the fresh fuel loading position. Therefore, fluence reduction in this part was focused on in this study.

3. Additional Shield installation for RPV Fluence Reduction

3.1. Reduction Effects Estimated by MCNP

To intensively mitigate the high flux of the weld at the RPV inner wall, additional shields were installed in the outer core structures. This strategy is not accompanied by the modification of fuel assemblies. For this reason, it is predicted that the core characteristics such as power distributions and peaking factors are influenced little by the alteration of outer core structures.

The shields were replaced in the coolant regions because the outer core structural components could not be conveniently removed or changed. The space of additional shields possibly inserted are between baffle and barrel, barrel and thermal shield (bypass), and thermal shield and vessel (downcomer). Shield type was divided into two classes : rod type and pad type. The rod type shields needed relatively more volume to be installed, and thus, was only applied to the space between baffle and barrel. However, the pad type shields could be installed at all spaces of the outer core owing to its simple geometry and small size.

The shield materials were chiefly used with stainless steel type 304 (SS-304) and tantalum (Ta). It is well recognized that SS-304 is a typical reactor material and an effective neutron scatterer so that a significant number of fast neutrons are reflected back into the core. Tantalum is also an effective neutron remover widely used to fabricate nuclear reactors. In addition, tantalum is said to have desirable

Table 1. Various Configurations of the Shields

Location		Geometry	Material	Specific Design Parameters
Baffle-Barrel	Outer Baffle Surface	Simple Pad	SS-304 Tantalum Graphite	Thickness : 1.5~3.0cm
	Between Baffle and Barrel	Solid Rod	SS-304 Titanium Tantalum Zircaloy-4 Borated SS	Rod Diameter : 0.9cm, Rod Pitch : 1.4cm
		Hollow Rod		Same Diameter and Pitch of Fuel Rod Rod Thickness : 1.0~4.0mm Inner Part of Rod : Polyethylene, Coolant
	Inner Barrel Surface	Simple Pad		Thickness : 1.0~2.5cm
		Repeated Pad		Thickness : 0.2cm, 0.4cm 3~5 Repeated Pads with Water
Bypass	Outer Barrel Surface	Simple Pad	Tantalum	Thickness : 1.9cm
	Inner Thermal Shield Surface	Simple Pad		Thickness : 1.9cm
Downcomer	Outer Thermal Shield Surface	Simple Pad		Thickness : 1.8cm
	Between Thermal Shield and Vessel	Simple Pad	SS-304 Titanium Tantalum Zircaloy-4 Lithium-6 Borated SS	Thickness : 2.0cm
		Repeated Pad		Thickness : 0.2cm, 0.4cm 3~5 Repeated Pads with Water
	Inner Vessel Surface	Simple Pad		Thickness : 1.0~5.0cm
		Repeated Pad		Thickness : 0.2cm, 0.4cm 3~5 Repeated Pads with Water

properties such as a high melting point, high strength, and good ductility. Moreover, many materials that are known as effective neutron absorbers and scatterers such as polyethylene, borated stainless, zircaloy-4, steel, lithium-6, graphite, and titanium were tested for fast neutron shielding. Table 1 lists locations, geometries, and materials of the shields tested in this work.

In the case of the rod type shields, two kinds of rods were used : solid rod and hollow rod. The inner part of the hollow rods was made such that it was filled with the coolant or the polyethylene. In general, the hollow rods filled with the coolant showed better effects on fast neutron fluence reduction than the solid rods and the hollow rods filled with the polyethylene. The rod type shield reduced the RPV fluence somewhat for all azimuthal angles, while for the high-flux region (at 0 degree) the effect of reduction was relatively poor. The pad type shields were placed along the outer core structures such as baffle, barrel, and thermal shield. To reduce the maximum fluence around 0 degree of azimuthal angle, partial pad was installed only between 0 and 15 degrees of core azimuthal angles. Repeated pads which are repeated with the coolant were also tested.

Through the various shield configurations, the several cases for effective neutron removing were found as follows :

Case 1. Hollow Ta rods type shield in baffle-barrel region - 2mm and 4mm rod thickness (Figures 6 and 7).

Case 2. SS-304 and Ta pads on outer baffle surface-2.9cm thickness (Figures 8 and 9).

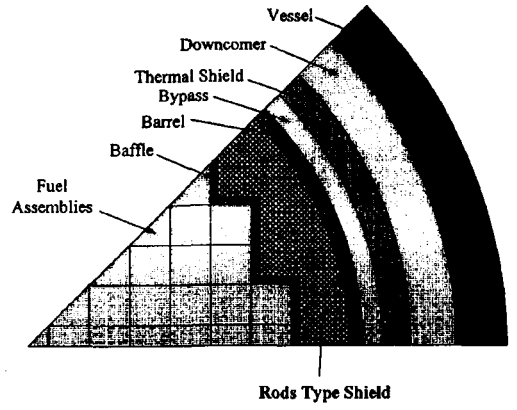

Fig. 6. Cross-Sectional View of the Rod Type Shield in Baffle-Barrel Region

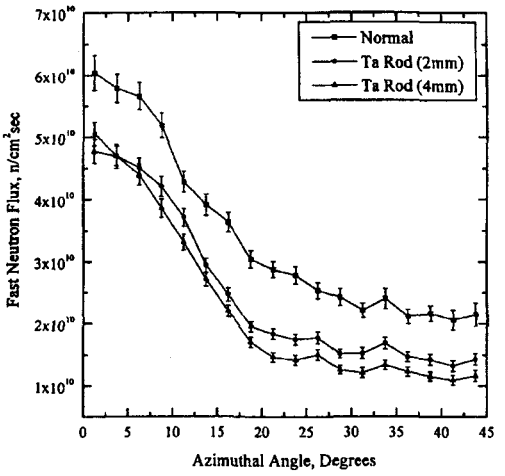

Fig. 7. Angular Fluence Distribution of Ta Rod Type Shields

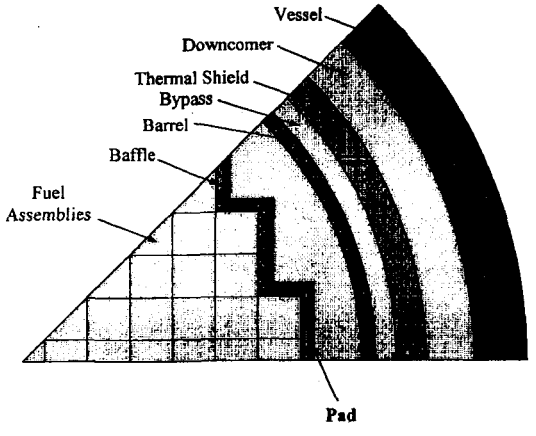

Fig. 8. Cross-Sectional View of the Pad Type Shield on Outer Baffle Surface

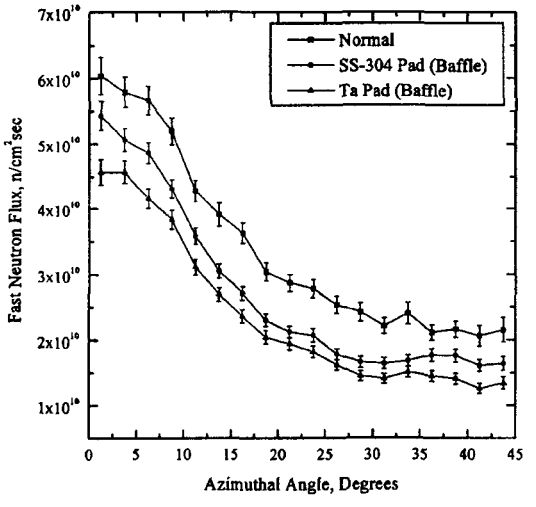

Fig. 9. Angular Fluence Distribution of SS-304 and Ta Pads On Outer Baffle Surface

Case 3. Three repeated pads of SS-304 and Ta on inner barrel surface - 0.4cm thickness per pad (Figures 10 and 11).

Case 4. Two Ta partial pads on outer baffle and barrel surfaces - 1.4cm and 1.9cm thickness (Figures 12 and 14).

Case 5. Three Ta partial pads on outer baffle, barrel and thermal shield surfaces - 1.4cm, 1.9cm and 1.8cm thickness (Figures 13 and 14).

In the case of shield installation in the downcomer region alone, the RPV fluence was somewhat higher than that of the reference case. Other materials except SS-304 and tantalum had little effect on the reduction of fast neutrons. It is regarded that these materials have a specific

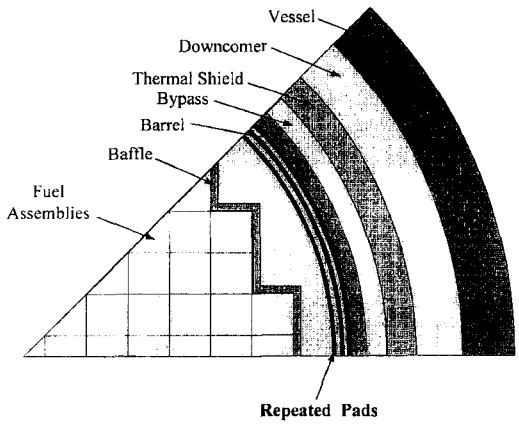

Fig. 10. Angular Fluence Distribution of SS-304 and Ta Repeated Pads Cases

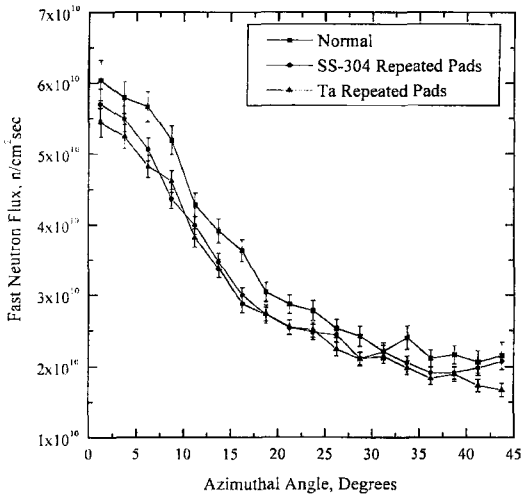

Fig. 11. Angular Fluence Distribution of SS-304 and Ta Repeated Pads Cases

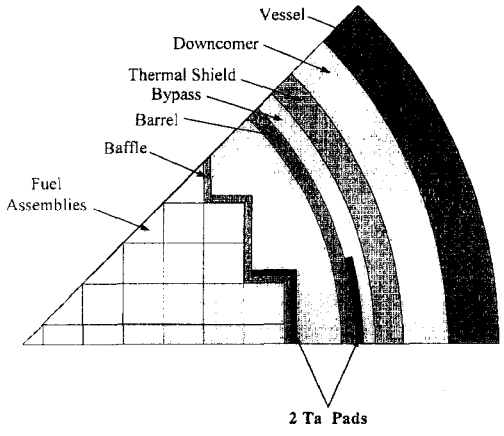

Fig. 12. Cross-Sectional View of the Two Ta Partial Pads Installation

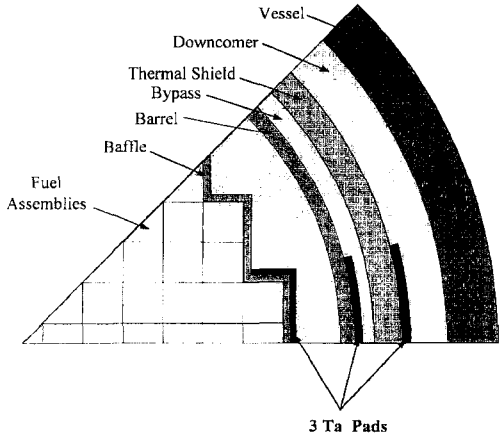

Fig. 13. Cross-Sectional View of the Three Ta Partial Pads Installation

energy range for effective fast neutron removing, but in the reactor core, there are neutrons having continuous energies over a wide range.

3.2. An Optimum Shield

Among the five effective shields, the case 5 with the three Ta pads most efficiently reduced the high-flux of the weld, and thus, this case was selected as an optimum shield in this study. The maximum fluence and the total fluence were reduced by 39% and 19%, respectively. In section 4, core nuclear characteristics and thermal hydraulic factors varying with the outer

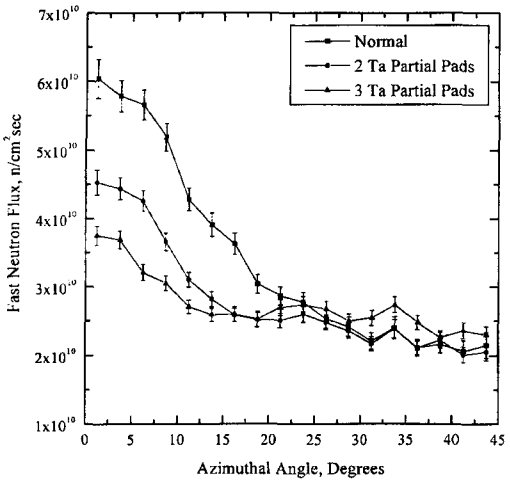

Fig. 14. Angular Fluence Distribution of Ta Partial Pad Cases

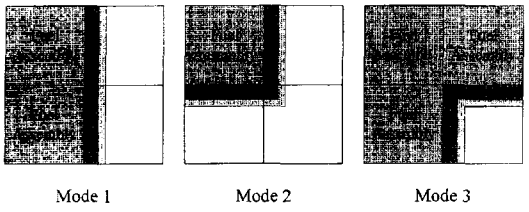

Fig. 15. Three Color Sets for the Homogenization Calculation

core modification were carefully examined, and so the additional life caused by fluence reduction can be predicted.

4. Evaluation of Vessel Integrity

4.1. Nuclear Characteristics Analysis

Installation of the Ta pads in outer core structures can change the core boundary conditions resulting in changes of power distribution and cycle length. However, there

	Kori Unit 1 with Ta Pad % Error*			0.767 0.701 -8.605			
D				1.110 1.109 -0.090	1.049 1.050 -0.095	0.609 0.607 -0.328	
E			1.135 1.136 +0.088	1.139 1.138 -0.084	1.048 1.048 0	0.803 0.774 -3.611	
F		1.093 1.093 0	1.103 1.103 0	1.130 1.131 +0.088	1.151 1.154 +0.261	1.089 1.103 +1.286	0.652 0.664 +1.840
G	1.093 1.093 0	1.015 1.015 0	1.096 1.096 0	1.115 1.116 +0.090	1.126 1.130 +0.355	1.050 1.059 -0.857	0.824 0.802 -2.670
	7	8	9	10	11	12	13

* % Error = (Ta Pad-Normal) / Ta Pad × 100

Fig. 16. Change of Radial Power Distribution by Ta Pads(Kori Unit 1, Cycle-1)

will be no effects on safety parameters such as fuel temperature coefficient (FTC) and moderator temperature coefficient (MTC). Quite a few changes are expected in rod worths and shutdown margins due to the radial power distribution changes. In this study, therefore, only the effects on power peaking were assessed for the core with Ta pads. In order to check only the effect of the Ta partial pads insertion, the first cycle core of the Kori Unit 1 was tested instead of the reload cycle cores.

All homogenized 4 group constants and discontinuity factors were derived from three kinds of color sets which include fuel assemblies, baffle, Ta pads, and water reflector in the distinct configurations, as shown in Figure 15. Figure 16 shows the change of radial power distribution in the case of the Ta pads insertion. By virtue of the thinness of the Ta pad, radial power distribution was not changed greatly even though fast neutron fluence level was greatly reduced.

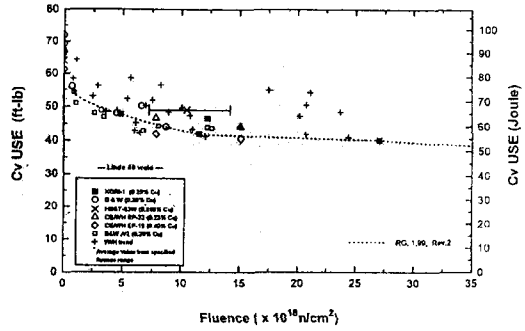

Fig. 17. Charpy USE of the Kori Unit 1 Weld Metal

4.2. Thermal Hydraulic Effect of Ta Pads Installation

In order to reduce fast neutron fluence at the weld of RPV of the Kori Unit 1, it was proposed to install Ta pads at the bypass flow channels, i.e., the spaces between the baffle and the thermal shield, and this can change the thermal hydraulic parameters. Assuming the space between the barrel and the baffle was fully filled with a metallic shielding pad, 0.7% increase of the core effective flow was estimated. Increment of the effective core mass flow rate can increase the departure from nucleate boiling rate (DNBR). One percent increase of the core effective flow increased about 0.7% DNBR, conservatively. Therefore, the installation of metallic shielding pads could increase DNBR, which was the positive effect of Ta shielding pads installation.

4.3. Analysis of Low Upper Shelf Toughness and Pressure Thermal Shock

Due to irradiation embrittlement, the RPV beltline material changes in the fracture toughness characteristics [16]. This can cause a failure of RPV during transients like loss of coolant accidents. To evaluate the reactor vessel integrity, U.S. Nuclear Regulatory Commission (NRC) provided regulations about the two following issues:

- Low Upper Shelf Toughness (LUST) [17,18,19]
- Pressurized Thermal Shock (PTS) [20]

The two issues above were studied to evaluate the RPV integrity of the Kori Unit 1 for the

Table 2. Results of Fracture Toughness Analysis of the Kori Unit 1 RPV(32EFPY 1/4t Fluence = 3.49×10^{10}n/cm^2)

(a) Level A/B Service Load : $J_{app} < J_{0.1}$

Criterion	J_{app} (SF=1.15)	J_R (0.1")	P_D	P_{crit} $J_{app}=J_{0.1}$	SF (P_{crit}/P_D)
Satisfied	93 lb/in	407 lb/in	2485 psi	7175 psi	2.9

(b) Level A/B Service Load : $\frac{\partial J_{app}}{\partial a} < \frac{\partial J_R}{\partial a}$ at $J_{app}=J_R$

Criterion	J_{app} (SF=1.25)	P_D	P_{crit}	SF (P_{crit}/P_D)
Satisfied	107 lb/in	2485 psi	7417 psi	3.0

(c) Level C Service Load : $J_{app} < J_{0.1}$

Criterion	J_{app} (SF=1.0)	J_R (0.1")	P_D	P_{crit} $J_{app}=J_{0.1}$	SF (P_{crit}/P_D)
Satisfied	289 lb/in	407 lb/in	2485 psi	4519 psi	1.8

(d) Level C Service Load : $\frac{\partial J_{app}}{\partial a} < \frac{\partial J_R}{\partial a}$ at $J_{app}=J_R$

Criterion	J_{app} (SF=1.0)	P_D	P_{crit}	SF (P_{crit}/P_D)
Satisfied	289 lb/in	2485 psi	4930 psi	2.0

(e) Level D Service Load : $\frac{\partial J_{app}}{\partial a} < \frac{\partial J_R}{\partial a}$ at $J_{app}=J_R$

Criterion	J_{app} (SF=1.0)	J_R (0.1")	P_D	P_{crit}	SF (P_{crit}/P_D)
Satisfied	371 lb/in	629 lb/in	2485 psi	6420 psi	2.6

extended operation period.

4.3.1. Low Upper Shelf Toughness Analysis

As a screening criterion, 10 CFR 50 App. G [19] requires the predicted value of upper shelf energy (USE) at the end of life to be higher than 50 ft-lb. Charpy USE of the Kori Unit 1 calculated from surveillance capsule data are shown in Figure 17 [21].

Charpy USE went down below the limiting value of 50 ft-lb in 1994, which corresponds to 11 effective full power years (EFPYs), and cumulated fast neutron fluence was 9.15×10^{18}n/cm^2. Because the screening criterion did not satisfy the reactor operation period, detailed plant specific fracture analyses according to the evaluation procedures given in ASME code section XI App. K were needed to ensure the RPV integrity [22]. The procedures can be summarized as follows :

- Reactor vessel flaws are postulated in accordance with ASME code section XI App. K-2000.
- Loading conditions at the locations of the postulated flaws are determined for Level A/B, C, and D service loadings.
- Material properties are determined at the postulated flaws.
- Applied J-integral for the postulated flaws is calculated and compared to the J-integral fracture resistance of the material.

Applied J-integral and the J-integral fracture resistance of the Kori Unit 1 were calculated and compared in accordance with the above procedures. The results are summarized in Table 2. In the table, SF is safety factor which represents safety margin. For all service loading conditions, the results show enough safety margins for fracture toughness requirements.

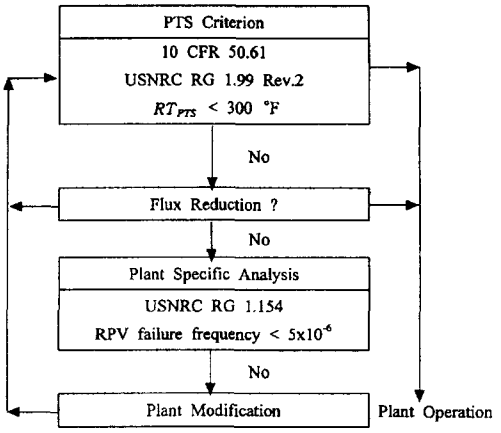

Fig. 18. Charpy USE of the Kori Unit 1 Weld Metal

4.3.2. Pressurized Thermal Shock (PTS) Analysis

To protect against pressurized thermal shock events, 10 CFR 50 proposed the pressurized thermal shock rule for calculating RT_{PTS}, the reference temperature that is to be compared to the screening criterion given in the rule [23]. The PTS screening criterion is the calculated RT_{PTS} to be lower than 300°F for circumferential weld of the Kori Unit 1 RPV. The PTS analysis procedures are shown in Figure 18.

The reference temperature RT_{PTS} is defined as follow :

$$RT_{PTS} = \text{initial } RT_{PTS} + \Delta RT_{PTS} + \text{Margin} \quad (1)$$

Detailed procedures to calculate rm initial RT_{PTS}, ΔRT_{PTS}, and Margin are given at 10 CFR 50.61 and U.S. NRC RG 1.99 Rev.2.

4.3.2.1. Initial RT_{NDT}

When generic mean data were used, initial

Table 3. Calculations of Initial RT_{NDT}, *CF*, and Margin

CASE	Initial RT_{NDT}	*CF*	Margin
Reference	-10.0°F	196.0°F	56.00°F
CASE 1	0.0°F	203.4°F	65.51°F
CASE 2	-10.0°F	203.4°F	56.00°F
CASE 3	-10.0°F	196.0°F	28.00°F

Table 4. Calculated RT_{PTS} in Case of No Ta Pads Installation

EFPY	Operating Year (Calendar Year)	ID Fluence 10^{19} n/cm^2	RT_{PTS}
11.5	14.3 (1994.7)	1.35	258.4
14.6	18.3 (1998.7)	1.70	270.6
21.8	27.2 (2007)	3.07	300.0
24.0	30.0 (2010)	3.49	305.9
32.0	40.0 (2020)	5.01	320.9

RT_{NDT} was 0°F for Linde 80 Flux. Otherwise when surveillance data were used, initial RT_{NDT} was -10°F according to the "Kori Unit 1 RPV radiation surveillance test program" of Westinghouse [21]. Recently, the adoption of nil-ductility temperature T_{NDT} from drop weight test as initial it RT_{NDT} was proposed by B&W based on the fracture toughness test results in the transition regions [24]. Nil-ductility temperature T_{NDT} of Kori WF232 weld was reported as -20°F according to the drop weight test.

4.3.2.2. ΔRT_{NDT}

Shift of RT_{NDT} due to irradiation was calculated from the following equation :

$$\Delta RT_{NDT} = (CF)\, f^{(0.28 - 0.10 \log f)} \qquad (2)$$

In Eq. (2), *CF* is chemistry factor which can be determined either from generic mean data or from surveillance data. When generic mean data were used, *CF* was 203.4°F for the Kori Unit 1 RPV belt line, where the weight percents of copper and nickel were 0.29 and 0.68, respectively. According to the surveillance data of the Kori Unit 1, *CF* was calculated as 196.0°F [21].

Table 5. RT_{PTS} in Case of Ta Pads Installation

EFPY	Operating Year (Calendar Year)	ID Fluence 10^{19} n/cm^2	RT_{PTS}
11.5	14.3 (1994.7)	1.35	258.4
14.6	18.3 (1998.7)	1.70	270.6
24.0	30.0 (2010)	2.81	295.9
26.2	32.7 (2013)	3.07	300.0
32.0	40.0 (2020)	3.76	309.2

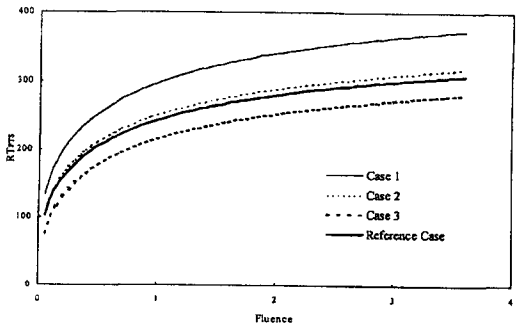

Fig. 19. Procedures of PTS Analysis

4.3.2.3. Margin

Margin was added to obtain conservative reference temperature and is given in App. G to 10 CFR 50 as,

$$\text{Margin} = 2\sqrt{\sigma^2_U + \sigma^2_\Delta} \qquad (3)$$

, where σ_U and σ_Δ are standard deviations of initial RT_{NDT} and ΔRT_{NDT}, respectively. When generic data were used for initial RT_{NDT} and ΔRT_{NDT} calculations, σ_U and σ_Δ was given as

17°F and 28°F, respectively. Margin is then given as 65.5°F from Eq. (3). If surveillance capsule data were used for initial RT_{NDT} then σ_U was given as 0°F. Also, when credible or incredible surveillance capsule data were used for ΔRT_{NDT}, then σ_Δ was given as 14°F or 28°F, respectively.

5. Predicted Lifetime Extension

As a reference case, initial RT_{NDT} was given as -10°F from surveillance data, and CF was given as 196.0°F according to the surveillance data of the Kori Unit 1, and Margin was given as 56.0°F by assuming that surveillance capsule data was incredible. Other 3 cases are also shown in Table 3. The reference temperature RT_{PTS} for several cases are shown in Figure 19 as a function of fast neutron fluence.

In the case of no Ta pads installation, RT_{PTS} will exceed the screening criterion in the year 2007, which is within the designed lifetime, as shown in Table 4 for reference case. In that case, detailed PTS analysis will be needed to ensure the RPV integrity.

When the proposed Ta pads are installed, fast neutron fluence is reduced considerably, and RT_{PTS} will exceed the screening criterion in the year 2013 as shown in Table 5. If the proposed Ta pads are installed, screening criterion will be satisfied within the designed lifetime. Table 5 shows that Ta pads are very effective in lowering the RT_{PTS}. In order to extend the reactor lifetime to the year 2020, however, a more effective fluence reduction program should be prepared in addition to Ta pads installation.

6. Conclusions

The computational model for RPV dosimetry was applied to the Kori Unit 1, the first Korean commercial nuclear plant, to quantitatively investigate the feasibility of lifetime extension. The fuel loading of cycle 14 was explicitly described by pin-by-pin with MCNP4A Monte Carlo code, and the validity of modeling was confirmed by criticality calculation. By using neutron source distribution from the criticality calculation, the RPV fluence was calculated around the high-flux weld region. Around 0 degree of core azimuthal angle, the fluence showed a peak value due to the core geometry and the fresh fuel loading position, therefore the study was focused on the fluence reduction at this high-flux region.

The strategy of additional shields insertion in outer core structures was applied to reduce the RPV fluence. After various geometries and materials were considered for the additional shields, an optimum shield which consists of three partial pads fabricated with tantalum was finally determined. The maximum fluence at the weld was reduced by 39%.

It was investigated that the core nuclear characteristics such as power distribution and peaking factors were little affected by the Ta pads insertion. The bypass flow reduction due to insertion of the pad type shield increased effective core mass flow rate, and thus, optimistically increased DNBR. The changes of other thermal hydraulic parameters such as coolant temperature and RCS pump loading were small enough to be neglected.

On the basis of fracture toughness requirements, so called Charpy USE and PTS criteria, the predicted lifetime extension of the modified core was calculated. By installation of the three Ta partial pads, 4.6 EFPYs of additional life was expected. It is expected that the results of this work will be easily applicable for analyzing the lifetime extension of other old reactors.

Acknowledgement

The authors would like to acknowledge full support for this work from the Electrical Engineering and Science Research Institute in Korea.

References

1. W. E. Pennel and S. N. M. Malik, "Structural Integrity Assessment of Aging Nuclear Reactor Pressure Vessels," *Nuclear Engineering and Design*, **172**, 27(1997).
2. D. Frankin and T. Marston, "Investigating the Flux-Reduction Option in Reactor-Vessel Integrity," EPRI-NP-3110-SR, Electric Power Research Institute, (1983).
3. Nuclear Energy Agency, "Computing Radiation Dose to Reactor Pressure Vessel and Internals," NEA/NSC/DOC(96)5, (1996).
4. J. C. Wagner, A. Haghighat, and B. Petrovic, "Monte Carlo Transport Calculations and Analysis for Reactor Pressure Vessel Neutron Fluence," *Nuclear Technology*, **114**, 373 (1996).
5. P. G. Laky and N. Tsoulfanidis, "Neutron Fluence at the Pressure Vessel of a Pressurized Water Reactor Determined by the MCNP Code," Nuclear Science and Engineering, 121, 433(1995).
6. R. Jeraj, B. Glumac, and M. Maucec, "Monte Carlo Simulation of the Triga Mark II Benchmark Experiment," *Nuclear Technology*, **120**, 179(1997).
7. E. L. Redmond II, J. C. Yanch, and O. K. Harling, "Monte Carlo Simulation of the Massachusetts Institute of Technology Research Reactor," *Nuclear Technology*, **106**, 1(1994).
8. S. N. Jahnhan and W. K. Terry, "A Comparison of Two Versions of a Proposed Test Reactor Using the MCNP Neutronics Code," *Nuclear Technology*, **110**, 93(1995).
9. J. O. Kim, "Evaluation of PWR Type Reactor Vessel Neutron Fluence by Monte Carlo Simulation," Ph.D Dissertation, Dept. of Nuclear Engineering, Hanyang University, Seoul, Korea, (1997).
10. Korea Electric Power Corporation, "Final Safety Analysis Report of the Kori Unit 1," (1976).
11. J. F. Briesmeister, "MCNP - A General Monte Carlo N-Particle Transport Code, Version 4A," LA-12625-M, Los Alamos National Laboratory, (1993).
12. M. Edenius and B. H. Forssen, "CASMO-3 A Fuel Assembly Burnup Program User's Manual, Version 4.4," STUDSVIK/NFA-89/3, (1989).
13. E. MacFarlane and D. W. Muir, "The NJOY Nuclear Data Processing System, Version 91," LA-12740-M, Los Alamos National Laboratory, (1994).
14. U.S. Nuclear Regulatory Commission, "Fracture Toughness Requirements for Light Water Reactor Pressure Vessels," 10 CFR Part 50, (1994).
15. J. Y. Kim, S. Y. Park, and J. W. Song, "Nuclear Design Report for Kori Nuclear Power Plant Unit 1 Cycle 14," KAERI/TR-443/94, Korea Atomic Energy Research Institute, (1994).
16. U.S. NRC, "Radiation Embrittlement of Reactor Vessel Materials," Regulatory Guide 1.99 Rev 2, (1988).
17. U.S. NRC, "Fracture Toughness Requirements for Light Water Reactor Pressure Vessels," 10 CFR 50, FRN0517.94., (1994).
18. A. Hiser, "Proposed Rule Package on Toughness Requirements for Light Water Reactor Vessels," (1993).
19. U.S. NRC, "Evaluation of Reactor Pressure

Vessels with Charpy Upper-Shelf Energy Less Than 50 Ft-Lb," Draft Regulatory Guide DG-1023, (1993).
20. U.S. NRC, "Fracture Toughness Requirements for Protection against Pressurized Thermal Shock," 10 CFR 50.61, (1997).
21. KAERI, "Integrity Assessment of Kori Unit 1 RPV for Lower Upper Shelf Toughness," KAERI/CR-005/94, (1994).
22. ASME, "Assessment of Reactor Vessels with Low Upper Shelf Charpy Impact Energy Levels," ASME Code Section XI, Appendix K, (1993).
23. U.S. NRC, "Format and Content of Plant Specific PTS Safety Analysis Reports for PWRs," Regulatory Guide 1.154, (1987).
24. B&W Technology, "Fracture Toughness Characterization of WF-70 Weld Metal," BAW-2202, (1993).